

Estimation of Blood Flow Speed and Vessel Location from Thermal Video

M. Garbey

A. Merla *

I. Pavlidis[†]

Computer Science Dept.
Univ. of Houston
Houston, TX 77204
garbey@cs.uh.edu

Computer Science Dept.
Univ. of Houston
Houston, TX 77204
amerla@mail.uh.edu

Computer Science Dept.
Univ. of Houston
Houston, TX 77204
ipavli@central.uh.edu

Abstract

In this paper we present a novel method for estimation of blood flow speed and vessel location from thermal video. The method is based on a bioheat transfer model that reflects the thermo-physiological processes in a skin region proximal to a major vessel. The model assumes the form of a partial differential equation (PDE) with boundary conditions. Initially, we test the soundness of our model by performing direct numerical simulation. Then, we solve the inverse problem both in steady and dynamic states on data provided by a thermal imaging system. Our method opens exciting possibilities in biometrics and biomedicine. Among others, it promises to revolutionize polygraph examinations by eliminating wiring and improving accuracy. It also establishes the feasibility of continuous 2D physiological monitoring of human patients in a contact-free manner.

1. Introduction

We have shown in a sequence of papers that analysis of thermal imagery holds great promise both for polygraph purposes [1, 2, 3] and for biomedical applications [4, 5, 6]. There are several advantages to this method:

1. It is a touchless technique. This is very important in the context of physiological measurements where it is crucial that the subject feels as comfortable as possible. Examples include the cases of polygraph tests or continuous physiological monitoring of patients.
2. After appropriate processing, the thermal imagery can yield quantitative information about variables other than temperature, like blood flow speed, respiratory, and perspiratory function. These variables provide information similar or complementary to that of traditional polygraph channels [3, 5]. They also constitute

*Currently on leave from the Dept. of Clinical Sciences & Bioimaging University "G. D'Annunzio," Chieti, Italy and the Istituto Nazionale Fisica della Materia, Coordinated Group of Chieti, Italy.

[†]To whom all correspondence should be addressed.

a set of vital signs, suitable for monitoring patients with cardiac or other problems. As opposed to traditional physiological measurements, all these variables can now be extracted from a single sensing regime and provide 2D information.

In this paper we focus on the computation of blood flow properties in vessels proximal to the skin. We use thermal video as the only source of data. Most other methods operate on data provided by thermistors or some type of contact sensing, like Doppler ultrasound probe.

Since we are interested in bioheat transfer describing the heat processes in the first few millimeters below the surface of the body, the vascularity of the underlying tissue cannot be neglected. Several models have been proposed in the past to address this problem. We refer to [7] for a general discussion on bioheat transfer processes and models, and to [3] for the general background on the computation of perfusion rate in skin with an underlying dense vascular structure. The legacy models can be decomposed roughly into two categories:

Continuum Models These models relate the blood perfusion rate to the temperature as a function of the effective conductivity of the tissue and the source of heat in the body core [3, 8, 9, 12]. Continuum models fail to take into account the heterogeneity of tissues as well as the position and shape of large vessels.

Geometric Models These models are based on the exhaustive description of the geometry of the vascular system, which accounts for all local variations of the temperature near the individual vessels [10, 11]. They cannot be easily generalized because of the great complexity and variability of the vasculature in the tissue layers under the skin.

In the context of bioheat modeling one can formulate several mathematical problems. **A mathematical problem of interest is to retrieve the vessel location as well as the blood flow speed for a given vessel proximal to the skin,**

from the thermal imagery that provides the skin temperature over time. In real life applications we may not have enough data to solve this problem and the data may be noisy. This paper presents a general procedure to solve the problem by recovering missing information on vessel morphology and blood flow fluctuations. The proposed method is novel in the sense that it does not conform neither to the continuum nor to the geometric paradigms, but it attempts to marry the advantages of both. Our method can be used both in polygraph and biomedical applications.

In Section 2 we introduce the model and identification parameter problem. In Section 3 we present our methodology in some detail. In Section 4 we conclude the paper and discuss our future plans.

2 Overview of the Model

Our model describes heat transfer in the vicinity of a large vessel proximal to the skin. We assume that the vessel acts as a volumetric heat source for the surrounding four-layer tissue structure. These layers are successively, in positive z direction, the skin, the fat, the muscle, and the core (see Figure 1). We also assume that each layer is isotropic with respect to thermal conductivity $K(z)$, metabolic heat rate $q^M(z)$, density ρ , and specific heat c of the tissue. The heat effect of the vessel on the skin temperature depends on the vessel's location and shape as well as the blood flow speed and temperature.

We consider a single large vessel running along the x direction without traversing across the y direction (see Figure 1). An example of a major vessel proximal to the skin is the radial vessel of the wrist (see Figure 2). The thermal conduction in the tissue surrounding the vessel is dominant in directions parallel (x) and perpendicular (z) to the skin. We can neglect heat transfer along the (y) axis because of the presence of other vessels, periodically arranged and similar to that considered. Therefore, our 2D model assumes the following form:

$$\rho c \frac{\partial \Theta}{\partial t} - \frac{\partial}{\partial x} (K(z) \frac{\partial \Theta}{\partial x}) - \frac{\partial}{\partial z} (K(z) \frac{\partial \Theta}{\partial z}) = q^{BL}(x, z) + q^M(x, z), \quad (x, z) \in (0, L) \times (0, D), \quad (1)$$

where q^M is the volumetric metabolic heat while q^{BL} is the heat due to blood flow speed u_{bl} in a vessel assimilated to a line source $z = S(x)$. $K(z)$ is the thermal conductivity of a particular layer, while ρ and c are the tissue density and specific heat respectively.

We impose the following boundary conditions:

$$\Theta(x, D, t) = \Theta_{core}, \quad x \in (0, L), \quad (2)$$

$$\Theta(x, 0, t) = \Theta_{skin}(x, t), \quad x \in (0, L), \quad (3)$$

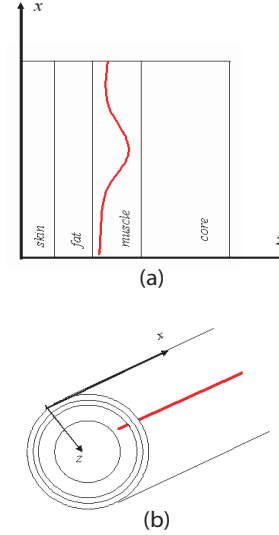


Figure 1: (a) Four-layer tissue structure hypothesized by our model along with the coordinate system convention. The red curve represents the assumed position and shape of the vessel. (b) Cross section of the tissue.

$$\frac{\partial \Theta}{\partial z}(x, 0, t) = \lambda (\Theta(x, 0, t) - \Theta_{air}) + q_{ir}, \quad x \in (0, L), \quad (4)$$

$$\frac{\partial \Theta}{\partial x}(0/L, z, t) = 0, \quad z \in (0, D). \quad (5)$$

λ is the convection heat transfer coefficient, which depends on air flow. According to [13]: $\lambda = 2.7 + 7.4 (v_{air})^{0.67} (W/m^2 K)$, where v_{air} is the air speed in (m/s). q_{ir} is the radiation heat flux: $q_{ir} = \sigma \epsilon (\Theta_{skin}^4 - \Theta_{wall}^4)$, where σ is the Stefan-Boltzmann constant and ϵ is the skin emissivity. Θ_{wall} is approximated by the temperature of the air.

The heat source term associated with blood flow is assumed to have the decomposition $q^{BL} = u_{bl}(t)r(x, z)$, where u_{bl} is the unknown blood flow speed in the vessel. We assume that the vessel is centered on the curve $z = S(x)$. Then, we take for $r(x, z)$ the modified bell function:

$$r(x, z) = \mu \exp\left(-\frac{(z - S(x))^2}{\pi \nu_{app}^2}\right).$$

ν_{app} is the apparent radius of the vessel seen as a heat source. μ is defined as follows:

$$\mu = \rho_{bl} c_{bl} \frac{A}{V} (\Theta_{vessel}(x, z, t) - \Theta(x, z, t)) \quad (J/m^4), \quad (6)$$

where ρ_{bl} and c_{bl} are the density and the specific heat of blood respectively, A is the vessel cross section, and V is the

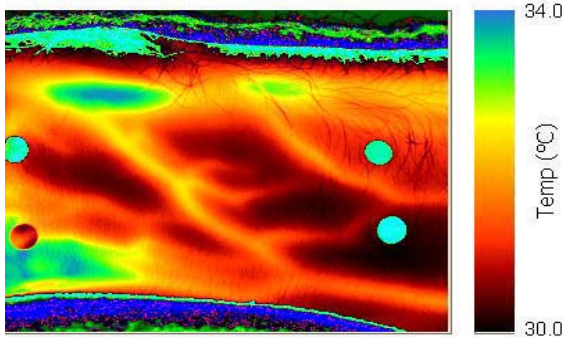


Figure 2: Thermal image of the wrist.

control volume of tissue. We assume that the temperature of the blood in the vessel is the same as the core temperature $\Theta_{vessel} = \Theta_{core}$.

In constructing our model, we have assumed that there is no heat flux between the domain of interest $(0, L) \times (0, D)$ with the rest of the body. The initial condition for the model will be defined later on.

The mathematical problem is to retrieve the unknown vessel location $z = S(x)$ and blood flow speed $u_{bl}(t)$ from the skin temperature Θ_{skin} obtained with an infrared camera.

3 Model Computation

We perform both direct simulation and solve the inverse problem. In each case we solve both the steady state and dynamic problems. To facilitate the solution we derive a normalized formulation of the model. The PDE of the normalized model is:

$$\frac{\partial \theta}{\partial t} - \frac{\partial}{\partial x} (\tilde{K}(z) \frac{\partial \theta}{\partial x}) - \gamma \frac{\partial}{\partial z} (\tilde{K}(z) \frac{\partial \theta}{\partial z}) = \tilde{\mu} u_{bl}(t) (1 - \theta) \exp\left(-\frac{(\gamma z - \tilde{S}(x))^2}{\eta}\right) + \tilde{q}^M(x, z), \quad (x, z) \in (0, 1) \times (0, 1). \quad (7)$$

$\tilde{\mu}$ and γ are normalization constants. The normalized boundary conditions are rewritten as:

$$\theta(x, 1, t) = 1, \quad x \in (0, 1), \quad t \in (0, T), \quad (8)$$

$$\theta(x, 0, t) = \theta_s(x, t), \quad x \in (0, 1), \quad t \in (0, T), \quad (9)$$

$$\frac{\partial \theta}{\partial z}(x, 0, t) = \beta \theta(x, 0, t), \quad x \in (0, 1), \quad t \in (0, T). \quad (10)$$

$$\frac{\partial \theta}{\partial x}(0, z, t) = \frac{\partial \theta}{\partial x}(1, z, t) = 0, \quad z \in (0, 1), \quad t \in (0, T). \quad (11)$$

This model becomes complete once we provide an initial condition $\theta(x, z, 0)$, where $x \in (0, 1)$ and $z \in (0, 1)$.

3.1 Direct Simulation in Steady State - 2D Model

For a known vessel location $\tilde{S}(x)$ and known blood flow speed $u_{bl}(t)$, we can obtain a well posed problem even when we drop boundary condition (9) or (10). We are going to present a direct simulation of the model by dropping boundary condition (9). Let us consider the steady state problem for $(x, z) \in (0, 1) \times (0, 1)$ and $\gamma = 1$:

$$-\frac{\partial}{\partial x} (\tilde{K}(z) \frac{\partial \theta}{\partial x}) - \frac{\partial}{\partial z} (\tilde{K}(z) \frac{\partial \theta}{\partial z}) = \tilde{\mu} u_{bl}(t) (1 - \theta) \exp\left(-\frac{(z - \tilde{S}(x))^2}{\tilde{\eta}}\right) + \tilde{q}^M(x, z), \quad (12)$$

with boundary conditions (8), (10), and (11).

This problem is well posed and has a unique continuous solution. The solution is C^1 but has second order derivative in the z direction with finite jump at the line of discontinuities $z = C^t$ of the thermal conductivity K . We use a Finite Volume (FV) approximation with centered cells of size $h_x \times h_z$ on a regular space grid. Let us denote $\theta_{i,j}$ the average value of θ in the centered FV cells. The discrete version of Equation (12) is:

$$-h_z (\Phi_{i+1/2,j} - \Phi_{i-1/2,j}) - h_x (\Phi_{i,j+1/2} - \Phi_{i,j-1/2}) = h_x h_z (\tilde{\mu} u(t)(1 - \theta_{i,j}) \exp\left(-\frac{(z_j - \tilde{S}(x_i))^2}{\tilde{\eta}}\right) + \tilde{q}^M(x_i, z_j)),$$

in the cell centered in (x_i, z_j) ,

$$x_i = h_x/2 + \frac{i-1}{N_x-1} h_x, \quad i = 1..N_x,$$

$$z_j = h_z/2 + \frac{j-1}{N_z-1} h_z, \quad j = 1..N_z.$$

The heat flux values at the wall of the cells are approximated with:

$$\Phi_{i+1/2,j} = K_{i+1/2,j} \frac{\theta_{i+1,j} - \theta_{i,j}}{h_x}, \quad i = 1..N_x - 1,$$

$$\Phi_{i,j+1/2} = K_{i,j+1/2} \frac{\theta_{i,j+1} - \theta_{i,j}}{h_z}, \quad j = 1..N_z - 1,$$

and

$$K_{i+1/2,j} = \frac{1}{2}(K_{i+1,j} + K_{i,j}), \quad K_{i,j+1/2} = \frac{1}{2}(K_{i,j+1/2} + K_{i,j}).$$

Using the boundary conditions on Φ and θ we obtain a classic linear system:

$$M \theta^{h_x, h_z} = \delta^{h_x, h_z}.$$

M is pentadiagonal matrix of size $(N_x \times N_z)^2$. θ^{h_x, h_z} is a matrix of size $N_x \times N_z$ reshaped from the 2D unknown solution's array $(\theta_{i,j})_{i=1..N_x, j=1..N_z}$ column-wise or row-wise. If $N_x < N_z$, we choose to reorder θ^{h_x, h_z} by column in order to minimize the bandwidth of the linear system: $Z = 2N_x + 1$.

Figure 3 shows a solution of the steady problem (12) with boundary conditions (8), (10), (11) and the vessel location given by the formula:

$$S(x) = 0.5 S_0 * (1 - \cos(2 \pi x)) + S_1. \quad (13)$$

We assume that the vessel is located in the muscle layer with parameter values $S_0 = S_1 = 0.2$. Figure 4 shows the sensitivity of the skin temperature as a function of the blood flow speed in the vessel. Figure 5 shows the sensitivity of the skin temperature as a function of the vessel's depth. These results are in qualitative agreement with our expectations. As a matter of fact, the skin temperature varies monotonically as a function of the vessel's depth z as well as its blood flow speed u_{bl} . Let us note that the skin temperature always stays bounded between the core temperature $\theta = 1$ and a minimum constant value corresponding to zero blood flow speed. We will denote this minimum value as θ_0 . Any dimensionless θ_{skin} obtained from thermal imaging outside the range $(\theta_0, 1)$ will be a strong indication that the parameter values of the model or the model itself are not relevant.

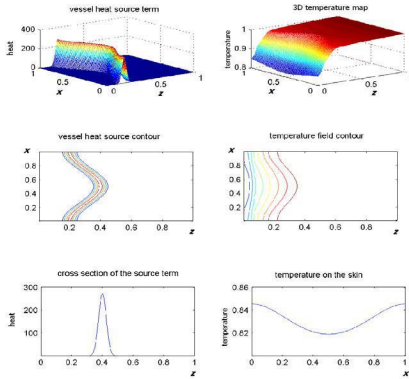


Figure 3: Steady state simulation: The top row shows on the left the vessel heat source q^{BL} and on the right the 3D temperature map. The middle row shows the corresponding contour plots. The bottom row shows on the left a cross-section of the heat source and on the right the spatial variation of skin temperature.

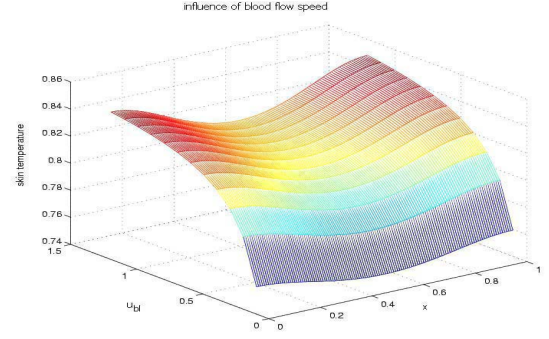


Figure 4: Influence of blood flow speed on the skin temperature in the steady simulation.

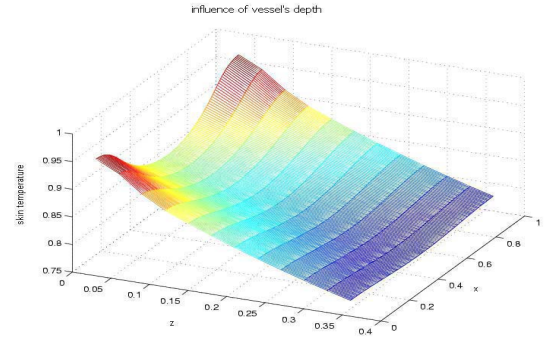


Figure 5: Influence of vessel's depth on the skin temperature in the steady simulation.

3.2 Direct Simulation in Steady State - 3D Model

Next, we develop a 3D model instead of a 2D. In the 3D case we consider a periodic solution in the y direction. The PDE of the 3D model is:

$$-\frac{\partial}{\partial x}(\bar{K}(z) \frac{\partial \theta}{\partial x}) - \frac{\partial}{\partial z}(\bar{K}(z) \frac{\partial \theta}{\partial z}) - \bar{K} \frac{\partial^2 \theta}{\partial y^2} = \tilde{\mu} u(t) (1 - \theta) \exp(-\frac{y^2}{\tilde{\eta}}) \exp(-\frac{(z - \tilde{S}(x))^2}{\tilde{\eta}}) + \tilde{q}^M(x, y, z), \quad (x, y, z) \in (0, 1) \times (0, 1) \times (0, 1), \quad (14)$$

with boundary conditions (8), (10), and (11) complemented with periodic boundary conditions in the y direction. Furthermore, the vessel is located on the line $y = 0, z = S(x)$. We take for \bar{K} an average value of the thermal conductivity,

$\bar{K} = 0.6$.

We construct our solution as a cosine expansion:

$$\theta(x, y, z, t) = \sum_{k=0..N_y} \theta_k(x, z, t) \cos(2\pi k \frac{y}{d}).$$

We can use a fast cosine transform to convert the vessel heat source q^{BL} from physical space to Fourier space at each time step. We use a semi-implicit scheme in time where q_{bl} is evaluated at the previous time step. The stability constraint on the time step is of the same order with what is required to get an accurate solution in our application, i.e., $dt \approx 1/31$.

With the same test case as in the 2D model, the computation of the 3D steady solution gives the skin temperature in the rectangle $(0, 1) \times (0, 1)$. Figure 6 reports on this solution. From the normalized variable θ , we can check that the temperature variation in the y direction is of the order of 10%, with the hottest points situated in the vertical sense.

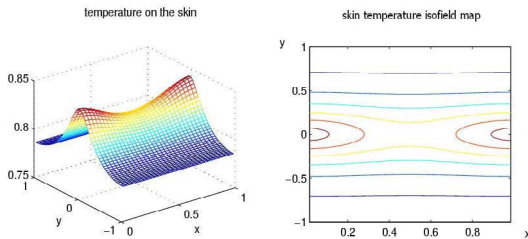


Figure 6: Temperature of the skin in the rectangle $(0, 1) \times (-1, 1)$ with a vessel located at $y = 0$.

3.3 Direct Simulation in Dynamic State

We compute the direct simulation in dynamic state with the same discretization in space as in the steady state case and a first order implicit Euler scheme in time:

$$\begin{aligned} \theta^{n+1} - \theta^n - dt h_z (\Phi_{i+1/2,j}^{n+1} - \Phi_{i-1/2,j}^{n+1}) - \\ dt h_x (\Phi_{i,j+1/2}^{n+1} - \Phi_{i,j-1/2}^{n+1}) = \\ dt h_x h_z (\tilde{\mu} u(t)(1 - \theta_{i,j}^{n+1}) \exp(-\frac{(z_j - \tilde{S}(x_i))^2}{\tilde{\nu}}) + \\ \tilde{q}^M(x_i, z_j)), \end{aligned} \quad (15)$$

where $\theta_{i,j}^n$ denotes the temperature at time n dt .

We keep the time step dt the same order as that of the space steps h_x, h_y . At each time step we have to solve a linear system with matrix $I_d - dt M$ to obtain θ^{n+1} . The matrix M is time dependent since the blood flow speed in

the vessel is time dependent. Therefore, we may use an iterative solver starting from the solution at the previous time step. Furthermore, the pre-conditioner does not need to be updated in all time steps.

In the dynamic direct simulation we are interested to compute the oscillations of the temperature on the skin as a function of the oscillating blood flow speed (cardiac cycle). We consider the following heat source term related to blood flow:

$$u_{bl}(t) = 1. + 0.3 * (\exp(-7 * \sin(\pi\omega t)^2) - 0.5).$$

We take $\omega = 1$ to simulate a cardiac pulse of 60 beats per minute. In our simulation we start with an initial condition that is the steady solution corresponding to the blood flow speed at $t = 0$.

The grid of computation is fixed to $N_x = N_z = 64$ and the time step is of the order of $1/31$, which corresponds to the time step between two frames in our thermal video. Figures 7 and 8 give a representative example of our dynamic direct simulation. We consider here the same parameter values as in the steady state example in Figure 3.

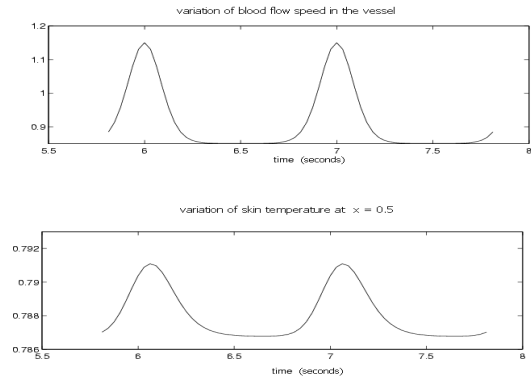


Figure 7: Skin temperature with pulsating blood flow in the vessel. The graph at the top shows the time variation of blood flow speed in the vessel. The graph at the bottom shows the time variation of skin temperature at location $x = 0.5$.

3.4 Inverse Problem

Initially, we solve our model in the steady state case. The steady state case solution provides the unknown position and shape of the vessel. Then, we use the steady state solution to solve the model in the time domain.

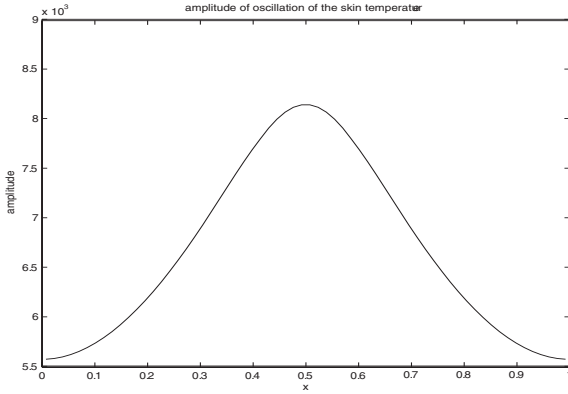


Figure 8: Amplitude of the skin temperature change with pulsating blood flow in the vessel. The graph shows the amplitude as a function of location x .

3.4.1 Inverse Problem in Steady State

The first step of the inverse problem procedure is to identify the average blood flow speed \bar{u}_{bl} and the location of the vessel $z = S(x)$, from the time average of the time dependent PDE model. Let us denote as $\bar{\theta}$ the average temperature in time. Since the PDE is linear, we get:

$$-\frac{\partial}{\partial x}(\bar{K}(z)\frac{\partial \bar{\theta}}{\partial x}) - \frac{\partial}{\partial z}(\bar{K}(z)\frac{\partial \bar{\theta}}{\partial z}) = \bar{\mu}\bar{u}_{bl}(1 - \bar{\theta}) \exp\left(-\frac{(z - \tilde{S}(x))^2}{\bar{\eta}}\right) + \bar{q}^M(z), \quad (x, z) \in (0, l_x) \times (0, 1), \quad (16)$$

with boundary conditions,

$$\bar{\theta}(x, 1) = 1, \quad x \in (0, l_x), \quad (17)$$

$$\bar{\theta}(x, 0) = \bar{\theta}_s(x), \quad x \in (0, l_x), \quad (18)$$

$$\frac{\partial \bar{\theta}}{\partial z}(x, 0) = \beta \bar{\theta}(x, 0), \quad x \in (0, l_x), \quad (19)$$

$$\frac{\partial \bar{\theta}}{\partial x}(0/1, z) = 0, \quad z \in (0, 1). \quad (20)$$

For reasons related to the optimization process that we will follow, we are interested to solve the problem in a space interval $x \in (0, l_x)$ that is no longer the unit interval. Let us denote $\theta_{observed}$ the skin temperature that we can retrieve from the thermal imaging camera.

In the PDE system (16), (17), (18), and (20) the unknowns are the average blood flow speed \bar{u}_{bl} and the vessel location $S(x)$. We can retrieve them by solving the minimization problem with the following objective function:

$$\|\bar{\theta}(x, 0) - \bar{\theta}_{observed}\|, \quad (21)$$

where $\|\cdot\|$ is the L_2 norm. Unless we know the average blood flow speed \bar{u}_{bl} the identification of vessel location $S(x)$ is an undetermined problem. We may constrain the optimization problem by assuming that \bar{u}_{bl} takes values in a given a priori estimated range $(u_{bl}^{min}, u_{bl}^{max})$ and by having morphological data on $S_{min} \leq S(x) \leq S_{max}$. For example, we know that the blood flow speed is in the range of $30 - 50 \text{ cm/sec}$ [20]. Furthermore, we know that the depth of the radial vessel is in the range of $3 - 4 \text{ mm}$, while the depth of the ulnar vessels is in the range $4 - 7 \text{ mm}$. Based on such data we assume that we have *a priori* a reasonable estimate of the average blood flow speed \bar{u}_{bl} and that the vessel of interest lays in the muscle layer.

The inverse 2D problem should have a moderate number of unknowns. In order to minimize the dimension of the search space we approximate $S(x)$ with a trigonometric polynomial:

$$S(x) = S_0 + \sum_{j=1..n} S_j \cos(j * \pi * x), \quad (22)$$

under the constraint $S_{min} < S(x) < S_{max}$. We may eventually assume a given decay of the sequence of coefficients $S_j \sim \frac{1}{j^p}$ assuming that the curve $z = S(x)$ is a $C^p(0, 1)$ function. We also observe that we have restricted ourselves to a vessel tangential to the skin at the end point, i.e., $S'(0/1) = 0$. This restriction is consistent with the zero flux boundary condition at the end point.

To facilitate the search on $S(x)$ we proceed with an increasing degree n of the trigonometric expansion in (22) with $1 \leq n \leq m$. First, we look at the horizontal line $S(x) = C$ for which we can match on average the observed skin temperature. Then, we look at the next order unknown term in the expansion, and so on. We can make the method more robust by starting from a $l_x > 1$ and decaying l_x until the correct value, if a solution exists. We implement this second procedure and use a Newton scheme to reach the objective (21). The Jacobian matrix is approximated using finite differences.

3.4.2 Inverse Problem in Dynamic State

In our application, we are mostly interested in the modulation of blood flow speed in time. The identification process of $S(x)$ with an a priori estimate of \bar{u}_{bl} can be seen as a first order correction to compensate for the small temperature variation on the skin along the length of the vessel (see Figure 9). We can now look for the even smaller temperature variation that is the consequence of the blood flow pulsation in the vessel.

Therefore, we use the vessel location derived from the time average skin temperature $\bar{\theta}_{observed}$ and a given frequency ω of the blood flow variation to get the amplitude of the blood flow pulsation.

Assuming that $u_{bl} = \bar{u}_{bl} + Pf(\omega t), t \in (0, T)$, with f a given periodic function of period $\frac{1}{\omega}$, we address the dynamic inverse problem, that is, to recover the amplitude of the signal P such that the skin temperature for the time periodic solution matches best the $\theta_{observed}(x, t)$. We have implemented this procedure using for the signal f a simple sinus wave, i.e.,

$$u_{bl}(t) = \bar{u}_{bl} + P \sin(\omega t).$$

The objective function to minimize is:

$$\|\hat{\theta}_{\omega} - \hat{\theta}_{observed,\omega}\|, \quad (23)$$

where $\hat{\theta}_{\omega}$ represents the coefficient in the trigonometric polynomial expansion of $\sin(\omega t)$. The solution of the dynamic inverse problem is straightforward, since we are dealing with the search of a single parameter.

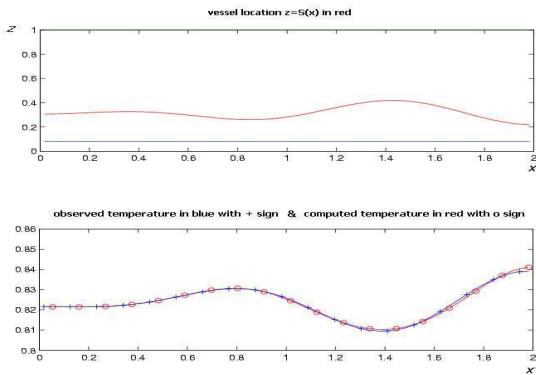


Figure 9: The solution of the inverse problem for the steady state model provides the vessel location (upper figure). In normalized coordinates, the vessel is located between $z = 0.2$ and $z = 0.4$, which corresponds to the muscle layer. The lower picture shows the experimental temperature profile over the skin atop of the vessel and compares it to the theoretical profile obtained by the model.

4 Conclusion

We have used thermal video to compute various parameters associated with blood flow. We have achieved this by capitalizing upon the physical meaning of the pixel values. In more detail, the thermal and dynamic properties of blood flow in large vessels are responsible for the control of the skin temperature. A general bioheat transfer model, aimed to describe the role of large vessels close to the skin, should take into consideration the geometry and the anatomy of the

tissue surrounding the vessel, its thermal properties, and the general energy balance between the vessel, the tissue, and the environment. Moreover, hypotheses about the location and the shape of the vessel should also be considered for a realistic description of the bioheat transfer processes. The model we propose tries to satisfy the above requirements since it starts from a general energy balance for the tissue surrounding the vessel, like in the Pennes' approach [8], but modifies the simplified Pennes' model as follows:

1. It takes into account a modified bell shape for the vessel. This shape formulation allows the model to adapt to arbitrarily complex vascular geometry.
2. It assumes a multi-layer structure for the surrounding tissue.
3. It assumes a modulation of the heat power of the vessel through its blood flow speed control.
4. It considers the vessel as a heat source, since its actual temperature is higher than the surrounding tissue.

Our work opens the way for multi-dimensional passive and remote physiological measurements which can run continuously on a subject. This may have a profound effect on psycho-physiology and preventive medicine. However, the present paper is methodological and offers validation only through simulation and limited laboratory testing. We are currently performing extensive clinical tests to further ascertain the experimental validity of our methods.

Acknowledgments

This research was supported by DARPA grant #N00014 - 03 - 1 - 0622, by TSWG subcontract #B09390131, and by the University of Houston start-up funds of Professor I. Pavlidis. The views expressed in this paper do not necessarily reflect the views of the funding Agencies.

References

- [1] J. Levine, I. Pavlidis, and M. Cooper, *The Face of Fear*, *The Lancet*, Vol. 357, No. 9270, June 2001.
- [2] I. Pavlidis, N.L. Eberhardt, and J. Levine, *Human Behavior: Seeing Through the Face of Deception*, *Nature*, Vol. 415, No. 6867, January 3, 2002.
- [3] I. Pavlidis and J. Levine, *Thermal Image Analysis for Polygraph Testing: Two-Dimensional Physiological Measurements Can Serve as an Additional Scoring Channel for Increased Accuracy*, *IEEE Engineering in Medicine and Biology Magazine*, Vol. 21, No. 6, pp. 56-64, November/December 2002.

- [4] I. Pavlidis, *Continuous Physiological Monitoring*, Proceedings of the 25th Annual International Conference of the IEEE Engineering in Medicine and Biology Society, Cancun, Mexico, September 17-21, 2003.
- [5] A. Merla, L. Di Donato, G.L. Romani, and P.M. Rossini, *Recording of the Sympathetic Thermal Response by Means of Infrared Functional Imaging*, Proceedings of the 25th Annual International Conference of the IEEE Engineering in Medicine and Biology Society, Cancun, Mexico, September 17-21, 2003.
- [6] A. Merla, L. Di Donato, P.M. Rossini, and G.L. Romani, *Infrared Functional Imaging Applied to the Study of Emotional Reactions: Preliminary Results*, Proceedings of the 4th International Non Invasive Functional Source Imaging Conference, Chieti, Italy, September 9-13, 2003.
- [7] H. Arkin, L.X. Xu, and K.R. Holmes, *Recent Developments in Modeling Heat Transfer in Blood Perfused Tissue*, IEEE Transactions on Biomedical Engineering, Vol. 41, No. 2, pp. 97-107, 1994.
- [8] H.H. Pennes, *Analysis of Tissue and Arterial Blood Temperatures in the Resting Human Forearm*, Journal of Applied Physiology, Vol. 1, pp. 93-122, 1948.
- [9] S. Weinbaum, L.M. Jiji, and D.E. Lemons, *The Bleed-off Perfusion Term in the Weinbaum-Jiji Bioheat Equation*, Journal of Biomechanical Engineering, Vol. 114, pp. 539-544, 1992.
- [10] J.W. Baish, P.S. Ayaswamy, and K.R. Foster, *Heat Transport Mechanisms in Vascular Tissues: A Model Comparison*, Journal of Biomechanical Engineering, Vol. 108, pp. 324-331, 1986.
- [11] S. Weinbaum, L.M. Jiji, and D.E. Lemons, *Theory and Experiment for the Effect of Vascular Microstructure on Surface Tissue Heat Transfer: Part I: Anatomical Foundation and Model Conceptualization*, Journal of Biomechanical Engineering, Vol. 106, pp. 321-330, 1984.
- [12] E.H. Wissler, *Pennes' 1948 Paper Revisited*, Journal of Applied Physiology, Vol. 85, pp. 36-42, 1998.
- [13] J. Werner and M. Buse, *Temperature Profiles with Respect to Inhomogeneity and Geometry of the Human Body*, Journal of Applied Physiology, Vol. 65, No. 3, pp. 1110-1118, 1988.
- [14] D. Gottlieb and Chi-Wang Shu, *On the Gibbs Phenomenon and its Resolution*, SIAM Review, Vol. 39, No. 4, pp. 644-668, 1997.
- [15] H. Brinck and J. Werner, *Estimation of the Thermal Effect of Blood Flow in a Branching Countercurrent Network Using a Three-Dimensional Vascular Model*, J. Biomech. Eng., Vol. 116, pp. 324-330, 1994.
- [16] M. Iwatani, *An Estimation Model of Skin Blood Flow Rate Using Heat Flow Analysis*, Jap. J. Medical Electron Biologic Engr., Vol. 20, No. 3, pp. 249-255, 1982.
- [17] Y. Jarny, M.N. Ozisik, and J.P. Bardon, *A General Optimization Method Using Adjoint Equation for Solving Multidimensional Inverse Heat Conduction*, Int. J. Heat Mass Transfer, Vol. 34, pp. 2911-2919, 1991.
- [18] K.H. Keller and L. Seiler Jr, *An Analysis of Peripheral Heat Transfer in Man*, Journal of Applied Physiology, Vol. 30, No. 5, May 1971.
- [19] J.C. Lagarias, J.A. Reeds, M.H. Wright, P.E. Wright, *Convergence Properties of the Nelder-Mead Simplex Method in Low Dimensions*, SIAM Journal on Optimization, Vol. 9, No. 1, pp. 112-147, 1998.
- [20] R. Joannides, A. Contentin, M. Iacob, P. Compagnon, A. Lahary and C. Thuillez, *Influence of Vascular Dimension on Gender Difference in Flow-Dependent Dilatation of Peripheral Conduit Arteries*, Am. J. Physiol. Heart. Circ. Physiol., Vol. 282, No. 4, pp. 1262-1269, 2002.
- [21] S. Weinbaum, L.M. Jiji, *A New Simplified Bioheat Equation for the Effect of Blood Flow on Local Average Tissue Temperature*, J. Biomech. Eng., Vol. 107, pp. 131-139, 1985.
- [22] S. Weinbaum, L.X. Xu, L. Zhu, and A. Ekpene, *A New Fundamental Bioheat Equation for Muscle Tissue: Part I - Blood Flow Perfusion Term*, J. Biomech. Eng., Vol. 119, pp. 278-288, 1997.
- [23] W. Wulff, *The Energy Conservation Equation for Living Tissue*, IEEE Trans. BME, Vol. 21, No. 6, pp. 494-495, 1974.
- [24] W. Wulff, *Alternatives to the Bioheat Transfer Equation*, Annals New York Acad. Sci., Vol. 335, pp. 151-154, 1980.